

Orbiting Wide-angle Light-collectors (OWL)

White Paper
Submitted to SEUS, Jan 31, 2002

Contributing Authors:

R. E. Streitmatter (Study Scientist)	<i>Streitmatter@lheavx.gsfc.nasa.gov</i>
Louis Barbier	<i>lmb@cosmicra.gsfc.nasa.gov</i>
John Krizmanic	<i>JFK@cosmicra.gsfc.nasa.gov</i>
Eugene Loh	<i>Loh@mail.physics.utah.edu</i>
John Mitchell	<i>Mitchell@milkyway.gsfc.nasa.gov</i>
Pierre Sokolsky	<i>ps@booboo.physics.utah.edu</i>
Floyd Stecker	<i>Stecker@twinkie.gsfc.nasa.gov</i>

OWL ROADMAP TO THE ULTRA-HIGH-ENERGY UNIVERSE

1. INTRODUCTION

The goal of the Orbiting Wide-angle Light-collectors (OWL) mission is to study the origin and physics attendant to the highest energy particles known in nature, the ultra-high-energy cosmic rays (UHECR). Results from AGASA and HiRes indicate that events exist well above the expected Greisen-Zatsepin-Kuz'min cutoff. The current set of ground-based detectors, operating and in construction, will be able to make excellent spectrum measurements around 10^{20} eV. However, to extend these measurements to a higher energy region where the cosmic ray origin may best be revealed will require a space-borne detector with a very large detection aperture and using the calorimetric technique. Experience indicates that a stereo (two satellite) detector complement with on-board calibration instrumentation providing observing aperture orders of magnitude greater than the current detectors is essential to the study of the highest energy cosmic rays.

2. SCIENCE GOALS

The scientific quest of the OWL mission can best be described by reference to the report of the National Research Council Committee on Physics of the Universe ('Turner Report'). The OWL mission will be able to address four of the eleven questions that are deemed to be fundamental to the science at the intersection of astronomy and physics.

We state these questions as rephrased by the Discover Magazine in its cover story of Feb. 2002:

Question 1. Where do ultrahigh energy particles come from?

The first puzzle relates to fundamental questions in both physics and astrophysics: *How can particles of energies eight orders of magnitude greater than the particles accelerated in man-made machines be produced? Are there any astronomical objects capable of accelerating particles to these energies in a so-called "bottom-up" process? Or, perhaps even more intriguing, are these particles produced in a "top-down" process, the end result of physics at an even higher energy scale, the scale at which the strong and electroweak forces of nature become unified? This energy scale, known as the GUT (grand unified theory) scale, is also the mass scale of predicted particles known as "leptoquarks" and "GUT Higgs bosons" that may be produced as the result of the annihilation or decay of relic "topological defects" formed in the very earliest stages of the big-bang as a result of a kind of "crystallization of the vacuum".*

Have these GUT scale particles produced ultrahigh energy neutrinos, photons and nucleons as a result of their decay? Theory predicts that the decay products will contain a large fraction of neutrinos and photons compared with hadrons. *OWL is capable of unique identification of ultrahigh energy neutrinos by measurement of air-cascade starting points deep in the atmosphere. If evidence for this is found, it will be our first tangible indication of the existence of a grand unification of three of the four forces of nature.*

The second puzzle can also have fundamental consequences for our basic understanding of high-energy physics: How can these ultrahigh energy particles reach us? These particles appear to be coming from all directions, not confined to the galactic plane and, indeed, the galactic magnetic field is too weak to contain them. This makes a strong case that they are coming from vast extragalactic distances. However, if that is the case, they should interact with the 400 photons per cubic cm of the cosmic 2.7K background radiation from the Big Bang, losing their energy by producing mesons, the so-called GZK (Greisen-Zatsepin-Kuz'min) effect. Because of these interactions, protons having "trans-GZK energies" above 100 EeV should not be able to reach us from distances greater than about 300 million light years, about 2 percent of the size of the visible universe. A "cutoff", i.e. sharp suppression of the spectrum, is expected as 10^{20} eV is approached.

The search for the GZK cutoff has been the holy grail of CR physicists since it was first proposed in 1967. While there were a number of hints of events beyond this cut-off in the 70's and 80's, it was not until publication in 1994 of the Fly's Eye monocular spectrum showing an exceptional event at 3×10^{20} eV, a factor of 5 greater energy than the predicted cutoff, that it became evident something extraordinary might be happening. The Fly's Eye fluorescence method is calorimetric and well calibrated. The HiRes experiment has recently observed 3 more events well above the GZK cutoff in very good agreement with the original flux estimated by the Fly's Eye. The AGASA ground array collaboration has also reported a significant number of events above 10^{20} eV, but with a larger spectral flux normalization. The ground array energy estimation is based on a very different non-calorimetric technique (the

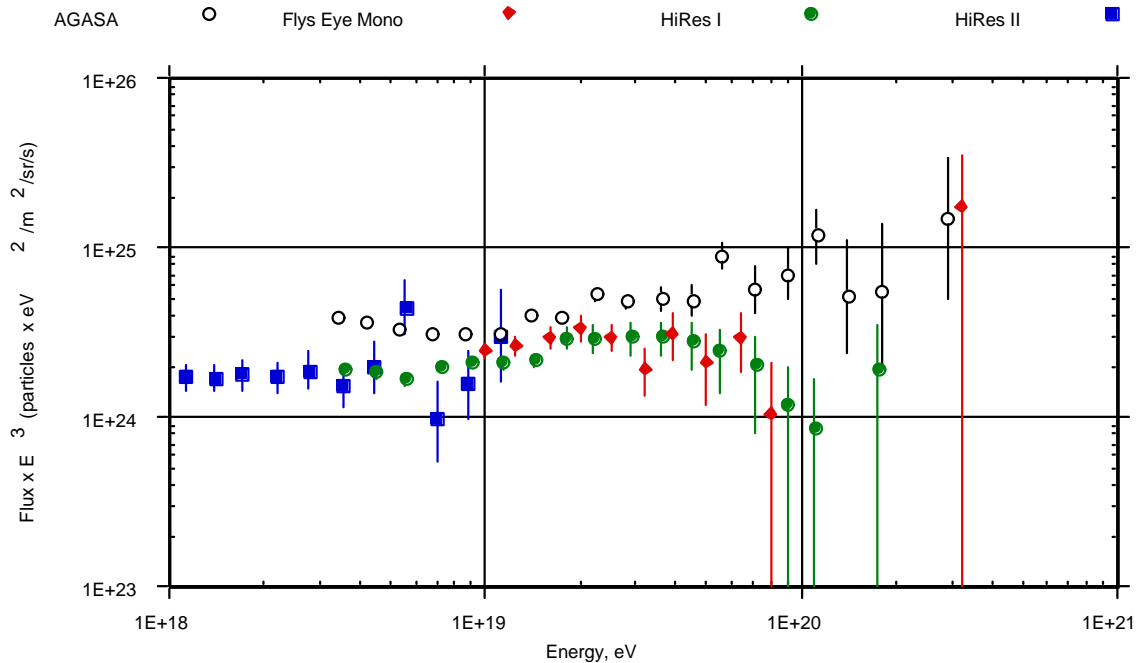


Figure 1

rho-600 method). There are likely systematic energy differences in the two techniques at the level of 20 - 40%. A 30% energy shift will bring the spectral normalizations of the two experiments into agreement above 10^{19} eV. In that case AGASA still reports about 5 events above 10^{20} .

Today, though the high-energy spectra from AGASA and HiRes still differ, there is agreement that events above the GZK limit exist. (See Figure 1.) There is no doubt that the difference, long thought to be accounted for by a combination of difference of energy scale and of energy resolution, will be solved by the Auger array being constructed in Argentina, where the fluorescence detector will examine 10% of the events measured by the sparsely-spaced ground detectors.

It should be noted that the UHECR spectrum may result from a combination of bottom-up and top-down processes. Noting an apparent gap in the UHECR spectra at about 10^{20} eV, Sigl, Lee, Schramm, and Bhattacharjee (1995) wrote ‘Persistence of the apparent gap in the data ... might hint to the existence of a “top-down” mechanism which produces an additional hard component of ultrahigh energy particles directly by decay from some higher energy scale in contrast to bottom-up acceleration of charged particles. *In this scenario a cutoff followed by a pronounced spectral flattening and possibly even a gap could be naturally formed.*’ Emphasis added.

OWL will answer the questions of the CPU report by observing potentially thousands of the giant atmospheric showers produced by the UHECR instead to the present handful of events, which is the result of decades of ground-based observations. In this way, *OWL can define the energy spectrum of these particles to energies approaching one percent of the GUT energy.* OWL can also explore the nature (composition) of the ultrahigh energy particles by studying the point of origin in the atmosphere and development of the showers that they produce. Even though these factors will fluctuate naturally from shower to shower, by measuring these factors for many showers, their average characteristics can be determined. Showers initiated by particles from top-down processes will not have heavy nuclei primaries, but a bottom-up origin may contain such nuclei.

Question 2. What is the dark matter?

As another “top-down” possibility, it has been suggested that the dark matter may consist of GUT scale supermassive particles with a long lifetime. These particles may slowly decay to produce the ultrahigh energy particles observed. Alternatively, it has been suggested that their annihilation in a dark matter galactic halo may produce the ultrahigh energy cosmic rays. *In either case, asymmetries in the distribution of dark matter will be reflected in a measured anisotropy of the ultrahigh energy cosmic rays measured by OWL.*

Questions 3 & 4. What is gravity? Are there additional dimensions?

These questions may be related because it has been suggested that the weakness of gravity compared to that of the other forces may be the result of a dilution caused by its propagation in extra dimensions which we do not directly experience in the macroscopic world. In such "Kaluza-Klein" type theories, the extra dimensions can result in extra degrees of freedom which allow neutrino cross sections to grow with energy to sizes approaching the scale of hadronic cross sections at ultrahigh energies. Ultrahigh energy neutrinos have been predicted to be produced by the decay of the mesons produced by protons interacting with the 2.7K radiation (GZK-Stecker neutrinos), by the GUT scale decay processes discussed above, and by the production of high-energy mesons in astrophysical sources such as quasars and gamma ray bursts. *By detecting ultrahigh energy neutrinos through the distinctive characteristics of the air showers which they produce, OWL can determine whether such an increase in the neutrino cross section exists at ultrahigh energies.* Only OWL will be sensitive enough to do ultrahigh energy neutrino studies. In this way, OWL can potentially shed light on the nature of gravity.

We add one additional question of fundamental significance:

Question 5. Does special relativity (exact Lorentz invariance) break down at ultrahigh energies? (This last question may be related to "What is gravity?")

One possible explanation of "how they get here from there" is to say that the energy sapping photomeson producing interactions expected to cut off the trans-GZK end of the ultrahigh energy cosmic ray spectrum is inoperative.

This would be the case if the energy threshold for these interactions were substantially above the value given by standard particle physics. Coleman and Glashow have shown that this will happen if Lorentz invariance is even very weakly broken at the highest cosmic ray energies observed. If so, this process will still occur at higher energies and should manifest itself *as a super-GZK cutoff, measurable by OWL.* The difference between the super-GZK cutoff energy and that predicted by standard physics -- the "weirdness factor" -- will then be a measure of how much deviation there is from exact Lorentz invariance. Because many recent quantum gravity scenarios (one cannot call them full fledged theories) predict deviations from exact Lorentz invariance, OWL can potentially shed light on the nature of gravity in this way also. (It was suggested that such a weirdness factor could be caused by a hadron containing a light gluino, however light gluinos have recently been ruled out by experiments at Fermilab.)

By addressing some of the "greatest unanswered questions in physics" today, the OWL mission can open up important new areas of research in both physics and astrophysics and stimulate the minds of the twenty-first century to new breakthroughs in our knowledge of the universe.

3.0 UHECR CALORIMETRY BY UV FLUORESCENCE

The Orbiting Wide-Field Light-Collectors (OWL) mission will provide the event statistics and extended energy range that are crucial to unraveling the UHECR mystery. To accomplish this, *OWL makes use of the Earth's atmosphere as a huge "calorimeter" to accurately measure the energy, arrival direction, and interaction characteristics of UHECR. A stereo measurement of atmospheric UV fluorescence produced by air shower particles is the most accurate technique that has been developed for measuring the energy, arrival direction, and interaction characteristics of UHECR.*

Air showers consist of huge numbers of charged particles produced by a cascade process in which the incident UHECR first interacts with the atmosphere and causes the emission of secondary particles. The number of particles in the shower multiplies through many subsequent interactions, reaches a maximum, and then diminishes as particle energies fall below the threshold for additional production. Through the cascade process, most of the energy of the primary UHECR is dissipated in the atmosphere.

The absorption of the primary particle energy by the atmosphere makes measurement of showers a calorimetric technique very similar to techniques used in high-energy accelerator and lower-energy cosmic ray measurements in which the particle energy is dissipated in a massive absorber and the energy deposited is measured. *The calorimetric technique for measuring particle energies and species is exceptionally well developed* due to its importance in high-energy accelerator experiments. Fully understanding the energy deposit in a calorimeter and identifying the primary particle requires measurements taken at many points during the shower development.

The details of the cascade process depend strongly on the species of the UHECR. However, in any case, some of the particle production results in an electromagnetic component (photons, electrons, and positrons) that progresses through successive generations of pair production and bremsstrahlung and dissipates energy by ionization of the atmospheric constituents. This, in turn, results in the emission of UV light from fluorescence of excited atmospheric nitrogen. *The fluorescence light from a cosmic-ray-induced air shower appears as a luminous disk, a few meters in depth with a radius less than a kilometer, moving through the atmosphere at the speed of light.*

For sufficiently high primary energies, some particles in the cascade, primarily electrons and positrons with some muons, survive to reach the ground. These particles can be measured by an array of detectors on the ground, providing a single "snapshot" of the shower. The Cherenkov light generated in the atmosphere by the shower passage can also be recorded by ground-based optical cameras as a measure of the number of particles in the shower. The interpretation of the ground array or Cherenkov results is highly dependent on Monte Carlo modeling. Neither of these techniques can adequately measure the details of shower development, and so fail to fully exploit the calorimetric technique.

A far more powerful, technique is to measure the UV fluorescent light generated by the shower. A fast, highly pixelized camera (or "eye") is used to resolve both the spatial and temporal development of the shower for all arrival directions except almost directly toward the camera (in which region it acts as a Cherenkov detector). This detailed information provides a powerful tool for determining the characteristics of the primary particle and the fluorescence technique is much less dependent on Monte Carlo modeling. The UV emission, principally in the 300 - 400 nm range, is isotropic and the camera can view the shower from any direction. This means that a single camera can view a hemisphere of sky, limited only by atmospheric absorption of the UV light and by physical interference. Thus, a single camera can provide a very large detecting volume. By placing the camera in space, the detecting volume can be vastly enlarged, limited mainly by the details of instrument design.

The fluorescence technique is the basis of the Fly's Eye and HiRes instruments and is employed by the Pierre Auger Array to help understand the systematics of its ground detector array and as input to its Monte Carlo model. Both monocular (Fly's Eye, HiRes I) and stereo (HiRes I+II) versions are possible. However, a single fluorescence camera images the projection of the shower onto a plane normal to the viewing direction. In monocular operation, precision measurements of the arrival times of UV photons from different parts of the shower track must be used to partly resolve spatial ambiguities. The angle of the shower relative to the viewing plane is resolvable using differential timing. Resolving distance, however, requires that the pixel crossing time be measured to an accuracy that is impossible to achieve in a real instrument. Stereoscopic observation completely resolves both of these ambiguities. In stereo, fast timing provides supplementary information to reduce systematics and improve the resolution of the arrival direction of the UHECR. The stereo view also confers the crucial advantage that differences in atmospheric absorption or scattering of the UV light can be flagged. The results obtained by the HiRes collaboration viewing the same shower in both modes have clearly demonstrated the superiority of stereo viewing. *The fluorescence technique, particularly in its stereo form, treats the atmosphere as a true fully active calorimeter from which the details of particle shower development can be accurately derived.*

4.0 MISSION CONCEPT

OWL employs a pair of formation-flying spacecraft in a low-inclination, medium-altitude orbit. The nearly nadir-pointing OWL instruments on each spacecraft view a common volume of atmosphere to observe UV light generated by particle showers resulting from the interaction of the incident UHECR with the Earth's atmosphere. OWL fully characterizes particle showers by using the two instruments in stereo to measure their detailed temporal and spatial development.

In more than thirty years of operation, only a few events with energies above 10^{20} eV have been observed by all of the large ground-based detectors. Thus, obtaining greater statistics and extending the observation to higher energies requires a collecting power at least thirty times greater than current arrays or detectors. The differential spectral index of high-energy cosmic rays is about -2.75 to -3.0. If the cosmic ray spectrum continues at this rate, an effective collecting power of $10^4 \text{ km}^2 \text{ sr}$ year (the nominal HiRes aperture for ten years) would yield perhaps 100 events above 10^{20} eV. These event statistics are marginal to allow any significant deviation, structure, or features between 10^{20} and 10^{21} eV to be resolved and a much larger effective aperture is needed. This is impractical to achieve on the ground. To answer this need, from 1000 km altitude *OWL views a "detector" area of over half a million square kilometers, giving an instantaneous aperture of $1.7 \times 10^6 \text{ km}^2 \text{ sr}$ if nadir viewing and $2 \times 10^6 \text{ km}^2 \text{ sr}$ in its usual off-nadir orientation.* OWL is only able to view the dark side of the Earth and its effective aperture is further reduced by the effects of the moon, man-made light, and clouds. Taking these into account, *OWL has a conservative effective aperture corresponding to $2.3 \times 10^5 \text{ km}^2 \text{ sr}$ in continuous operation.* While the best comparison of OWL to existing UHECR detectors would be the integral collecting power, the actual lifetimes of the ground arrays and of OWL are uncertain and the most valid comparison that can be made is the yearly collecting power. ***For each year of operation, OWL has 230 times the aperture of HiRes and 33 times the aperture of the Pierre Auger Array (330 times its most sensitive "hybrid" mode).*** In a nominal 3-year mission, OWL is expected to detect 2000 - 6000 events above 10^{20} eV if the UHECR spectrum continues unchanged.

5.0 OWL BASELINE INSTRUMENTATION

Since it was first proposed as a NASA "New Mission Concept" in 1996, OWL has been the subject of extensive trade and technical studies. These have examined all aspects of the instrument and mission. Most recently, in January 2002, the OWL instrument was the subject of a two-week study in the GSFC Instrument Synthesis and Analysis Laboratory (ISAL) and the mission was the subject of a one-week study in the GSFC Integrated Mission Design Center (IMDC). From these and preceding studies, a baseline has been defined for both the instrument and the mission. *The OWL baseline instrument and mission can be realized using current technology and OWL is not dependent on new technology development.*

5.1 Instrument Overview

The baseline OWL instrument, shown in Figure 2, is a large $f/1$ Schmidt camera with a 45° full field-of-view (FOV) and a 3.0 meter entrance aperture. The entrance aperture is filled with a Schmidt corrector. The deployable primary mirror is 7 meters in diameter. The focal plane has an area of 4 m^2 segmented into approximately 500,000 pixels distributed over 1300 multi-anode photomultiplier tubes. Each pixel is read out by an individual electronics chain and can resolve single photoelectrons. Taking obscuration by the focal plane and by the members supporting the focal plane and corrector plate into account, the effective aperture of the instrument is about 3.4 m^2 . A deployable light shield covers the instrument and a redundant shutter is used to close off the aperture during non-observing periods. A UV laser for atmospheric characterization is located at the back of the focal plane and fires through the center of the corrector plate to a small steering mirror system. Laser light reflected by clouds is detected and measured using the OWL focal plane.

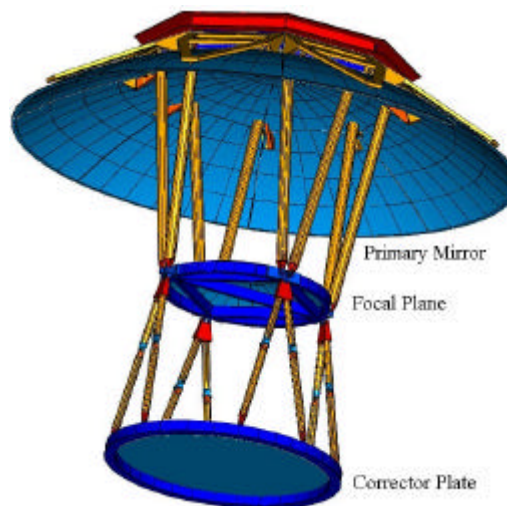


Figure 2

OWL is normally operated in stereo mode and the instruments view a common volume of atmosphere. However, the instruments are independent and the focal plane has been designed for a time resolution of $0.1 \mu\text{s}$ so that monocular operation can be supported (with reduced performance) if one instrument fails.

The instrument weight is estimated to be 1800 kg and total power consumption is about 600 W. The amount of data generated by the instrument is dominated by calibration and by atmospheric monitoring and averages 150 kbps over any 24 hour period.

5.2 Mission Overview

The satellites are launched as a dual manifest on a Boeing Delta IV Heavy (4050-H-19) into a 1000 km circular orbit with a nominal inclination of 10° . Figure 3 shows both satellites stowed in the Delta 4050-H-19 fairing. Following on-orbit checkout, the two satellites will fly in formation with a separation of 10-20 km for about 3 months to search for signatures of a special category of neutrinos that pass through the Earth and initiate upward-going showers. Following this period, the spacecraft separate to a 600 km for about 2.5 years to measure the high-energy end of the UHECR spectrum. Following this period, the altitude is reduced to 600 km altitude and 500 km separation to measure the cosmic ray flux above $5 \times 10^{19} \text{ eV}$. The choice of two different orbits is the result of a tradeoff among the collecting power, the angular FOV of the optical system, and the energy threshold of the instrument. The periods spent at each altitude and separation can be adjusted as instrument condition and detection results dictate. At the end of life, both satellites undergo controlled re-entry to minimize the risk from re-entering debris.

The instruments are approximately nadir viewing at all times but are pitched slightly so that they view common areas on the ground. During the 1000 km/600 km viewing period the leading instrument is pitched back 14 degrees and the trailing instrument is similarly pitched forward 14 degrees. Each instrument is completely shuttered whenever it might be exposed to direct or reflected sunlight or significant moonlight. Thus, the spacecraft can reorient to optimize solar panels and thermal radiator exposure and a simple single-axis solar array drive can be employed.

The OWL instruments function completely independently and event-taking does not require space-to-space communication. Events are triggered separately in each instrument using hierarchical hardware and software

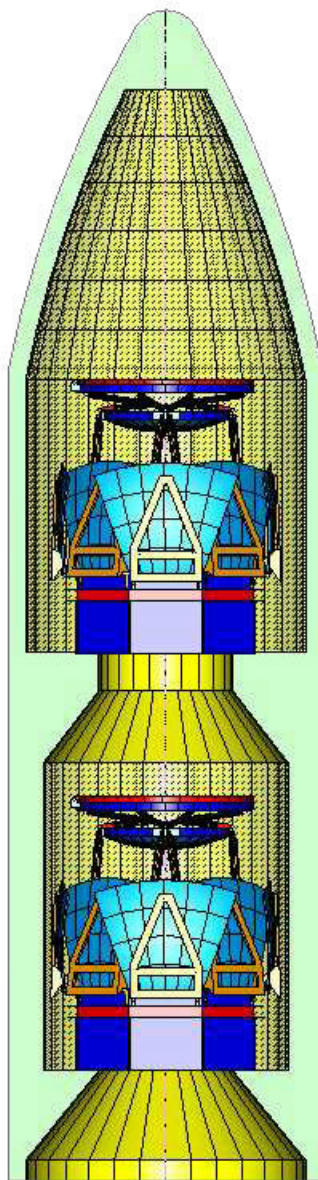


Figure 3

electrical and thermal services are routed. The corrector is carried by an extendable strut array from the edge of the focal plane structure. The entire optical system is covered by an inflatable light and micrometeoroid shield and is closed out by a redundant shutter system. The shield is composed of a multi-layer material with Kevlar layers for strength. It incorporates an inflatable toroidal support ring and strengthening/shaping ribs. These can be rigidized after inflation by the inclusion of UV or vacuum setting material. The full instrument/spacecraft with deployed shield is shown in Figure 4, where the shield has been made translucent to show internal structure.

algorithms to suppress background and localize shower tracks on the focal plane. A hardware trigger designed for very high efficiency and minimal dead time initiates acquisition in a limited region of the focal plane around the point where the trigger was generated. Subsequently, more selective hardware triggers and post-acquisition refinement of the viewed region and selection of events for telemetry limit the data volume telemetered without introducing significant efficiency systematics except near the detection threshold. In this way, all shower data acquired can be telemetered and no on-board data reduction is required. Data from both instruments is combined on the ground using GPS time stamps.

After an event location and crude track direction are determined by the trigger system a series of laser shots are taken along the track by each instrument to determine local atmospheric conditions in the region of triggered events. In addition, a random scan of the FOV is made at approximately one laser shot per second to characterize the average cloud obscuration. This is complemented by data obtained from geostationary and polar-orbiting IR-imaging satellites.

5.3 Optical System and Mechanical Deployment

Mass in the atmosphere is distributed exponentially with a scale height of about 8.6 km. As a result, cascade development and nitrogen fluorescence from most cosmic-ray-induced air showers occurs largely within a few tens of kilometers of the ground. Even at large zenith angles, the maximum extent of the showers is a several tens of kilometers. Thus, measuring the longitudinal profile of the cascade leads to a natural scale of about 1 kilometer. The corresponding optical angular resolution required depends upon the orbit altitude; e.g. observation from 1000 km implies an angular resolution of 1 milliradian, over 3 orders of magnitude larger than the diffraction limit.

The optical system is a low-resolution imager with more similarities to a microwave system than to a precision optical telescope. This allows the optical design to be simplified and has resulted in the selection of a simple, wide-angle (45° FOV), Schmidt camera design as shown in Figure 2. The Schmidt corrector has a spherical front surface and an aspheric back surface, while the primary mirror has a slight aspheric figure. The focal plane is a spherical surface tiled with flat detector elements.

The corrector is slightly domed for strength and is made in a segmented arrangement to simplify manufacture and test. The primary is made of lightweight composite material with a central octagonal section and eight petals which fold upward for launch. The petals are carried by A-frame structures with actuators for alignment. Four of the petals A-frames have simple hinges at the edges of the central octagon. Between each of these is a petal with an A-frame with an offset hinge so that it moves outward as it folds up. This allows the eight petals to be folded upward in a compact arrangement.

The focal plane is carried on a fixed array of struts, along which

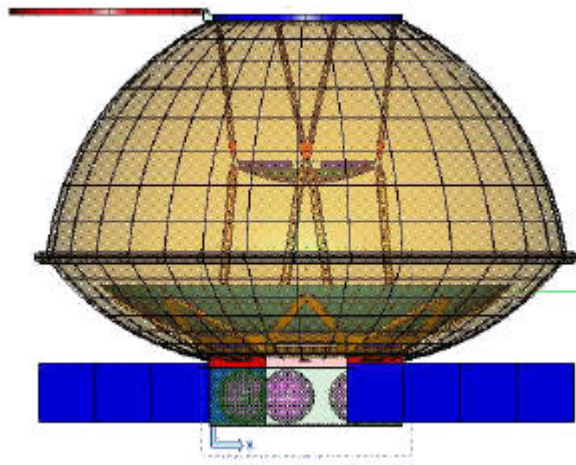


Figure 4

an intermediate point in the petal deployment. After activation of the focal plane and the instrument electronics systems, the petals are focused using the actuators on the A-arm to focus a point light source located at the center of curvature of the primary onto the focal plane.

5.4 Focal Plane, Trigger and Readout

The focal plane detector system has a total area of 4 m^2 divided into 5.4×10^5 pixels, each with an area of 7.4 mm^2 and able to detect ultraviolet light at the single photoelectron level. The dead area between pixels or groups of pixels is minimized both to maximize the detected signal and to insure that most showers will produce contiguous tracks. The detector and readout electronics measure incident light in $0.1 \mu\text{s}$ intervals to track the shower as it crosses the field of view of the pixel ($3.3 \mu\text{s}$ for a shower perpendicular to the viewing direction to cross 1 km). The timing information helps improve reconstruction systematics and angular resolution and supports potential monocular operation. The focal plane incorporates an absorption filter with a tailored bandpass between 330 and 400 nm to suppress optical background.

OWL requirements are best met by vacuum photomultiplier tubes (PMT) in which each pixel is an independent anode. Since the signal-to-noise ratio (S/N) will ultimately limit the lowest signal (and hence the lowest particle energy) that can be measured by OWL, devices which integrate background over many pixels are unsuitable. Single photoelectron detection requires the detector to have low intrinsic noise without extensive cooling. It also dictates that it should have a high intrinsic gain so that amplifier gain (with associated noise and power consumption) is minimized or eliminated. This effectively eliminates solid-state detectors and dictates the use of PMTs. These are historically the most important detectors for small light signals.

Multi-anode PMTs are in common use in astronomy, physics, and medicine and devices appropriate for OWL are under development by Burle Industries and Hamamatsu. In both cases, these are engineering developments based on existing technology. The Burle 85001 has an active area of 25 cm^2 and is based on a Z-stack microchannel plate multiplier with extensive space-flight heritage. The Hamamatsu H8500 is based on an etched metal foil dynode structure similar to R5800 PMTs

that have been flown on the STS. The Burle design is easily tailored to meet OWL requirements and a modified version with 400 pixels and a 36 cm^2 active area is baselined.

The instrument is launched with the primary mirror petals folded upward and latched, the corrector plate collapsed on the focal plane, some of the shield material pulled down into a storage volume below the mirror, and the shutter closed. This is shown in Figure 5, in which the shield has been omitted for clarity. The shield remains connected to the corrector plate ring at all times so that the instrument is always protected from ambient light.

After initial orbit acquisition, the instrument is deployed. This sequence is illustrated in Figure 5, 6 and 4, in order. First, the shield is inflated so that it is pulled out from the storage volume and separated from the other components of the instrument. A small positive pressure is generated in the shield volume and the support ring is fully inflated. Next, the corrector plate is raised into position and the ribs are inflated. These operations give the shield its final shape. The outer four primary mirror petals are then lowered into position and locked. Finally, the four inner petals are lowered and locked. Figure 6 shows

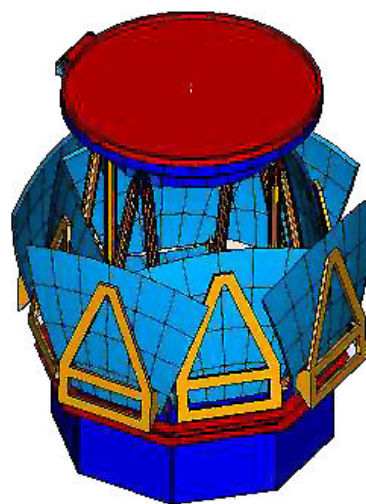


Figure 5

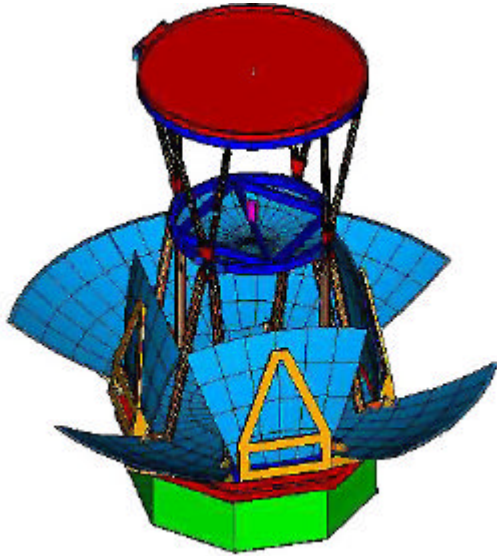


Figure 6

Both analog and photon counting approaches to the readout system have been considered. While photon counting is attractive it is not currently practical since the highest energy events expected by OWL would require counting at GHz rates. In the approach chosen as a baseline, the signal recorded by each pixel during a viewing interval (nominally 0.1 μ s) is delivered to a time-sliced analog storage device (e.g. switched capacitor array or SCA) as well as to the trigger electronics. The SCA acts as an analog ring buffer and digitization of the signal takes place only after an event trigger is received. The OWL SCA will be realized with 1 V (or lower) technology for low power consumption and each channel will incorporate 3000 SCA cells switching at 10 MHz. SCAs with more than 1000 cells and switching at 40 MHz are in use in large accelerator experiments. Showers can be detected over a radius of 60 km around the point at which a trigger is generated. The 300 μ s storage range of the SCA in effect covers a 30 km distance before the trigger point and 60 km after it. Thus, the trigger can be generated at any point from the start of a shower to its midpoint. Triggers are generated at the PMT level and a look-up table is used to identify all PMTs in the viewed region. Unless a higher-level hardware trigger stops the process, the SCAs in the

viewed region are stopped after 200 μ s and read out.

For input to the UHECR event trigger, signals from each pixel are integrated with a 3.3 μ s time constant to maximize the effective S/N and then fed to discriminators. These have adaptive thresholds that adjust automatically for variations in the background light and are set to a selectable value of about 7 times the integrated background. The discriminator outputs are applied to a logic array configured to examine the spatial and temporal topology around a triggered pixel for a selected number (typically 3-4) of pixels and pixel crossing times. In the presence of the nominal background of about 0.18 photoelectron/pixel- μ s this first-level trigger fires at about 35 Hz and engages less than 3 % of the focal plane each time. Thus, the effective trigger rate in any region is about 1 Hz, a rate easily supported by the data acquisition. Initial post-acquisition event selection takes place within 2 sec of a trigger and an initial determination of track direction is made to enable the laser to slew to that location and scan the atmosphere.

A parallel trigger system is provided for upward-going neutrino events. The pixel signals are applied directly to discriminators without integration so that the fast response of the photo detector can be exploited. As with the UHECR system, these have adaptive thresholds. Neutrino events are triggered if 2 adjacent fast discriminators go over threshold within a 50 nsec interval. If more than 16 discriminators exceed threshold in the same interval then the event is vetoed. After digitization, additional software selection is applied to eliminate anomalous events. Because only a small number of pixels and a small number of time slices at each pixel are involved in neutrino events, the amount of data generated is small and a relatively high false trigger rate can be tolerated. Combining data from the two satellites on the ground allows selection of the real neutrino events. The neutrino trigger can be disabled when the satellites are separated beyond the dimensions of the Cherenkov light pool.

The electronics system is based on low-voltage technology to limit power consumption. Estimated power consumption of the focal plane is between 360 and 470 W depending on PMT high-voltage requirements. The thermal load of the focal plane and laser is carried by two loop heat-pipes to radiators located on the satellite bus.

5.5 Atmospheric / Cloud Monitoring

Events observed by OWL will occur in an enormous footprint (size of the state of Utah) moving across the globe at a speed of 7 km/sec. The footprint will include variable amounts of clouds with altitudes from sea level to 15 km and variable boundary layer aerosols. Most extensive air showers will lie below 10 km. Consistency between the stereo views of an event provides a powerful tool for understanding whether the profiles of individual events have been altered by scattering through intervening high clouds or aerosol layers. In addition, OWL will use a steerable UV laser beam to scan the region of the event as a simple altimeter for cloud heights to provide real-time characterization of the atmosphere.

In order to normalize the observed event rate and calculate a flux OWL must characterize its instantaneous available aperture. OWL will use complementary approaches. While it is impractical to use the OWL laser to fully map the atmosphere, it will be used to provide a sparse scan of the full FOV. Accumulated over many viewing

passes, this information will provide an excellent statistical basis for understanding the aperture. This information will be complemented by geostationary and polar-orbiting IR satellite data to characterize the "clear-pixel" fraction in the detector aperture. Multi-wavelength IR signatures and the time dependence of IR emission in a given pixel have been shown to be effective signatures for determining the absence of significant clouds in a particular pixel. This technique has been used, in particular, to characterize aerosol distributions around the globe from IR and visible satellite data.

OWL is already a massively capable UV detector and monitoring clouds in the FOV of OWL requires only the addition of a UV laser. Based on designs developed for the GLAS (Geoscience Laser Altimeter System) mission, this is a diode-pumped Nd:YAG laser with about 75 mJ output at 1064 nm. Third-harmonic generation is used to obtain a 355 nm beam with an energy of about 15 mJ, a pulse duration of 5 nsec and an emittance of about 1 milliradian. The performance of the OWL optical system may allow the laser energy and beam purity to be reduced considerably from this baseline. The laser is located on the back (Earth viewing) side of the OWL focal plane so that it can share electrical and thermal services. It fires through an optical flat in the center of the corrector plate to a small steerable mirror system capable of slewing to any point in the OWL FOV in less than one second. The laser free runs at about 10 Hz and each laser shot is tagged with the firing time and instantaneous position of the mirror. After an event is triggered, the mirror is driven to the location of the track (taking into account orbital motion) and a scan along the track is carried out. At other times, the laser carries out a scan of FOV.

During the OWL mission life, it is expected that the laser will fire on the order of 10^9 times. YAG lifetimes of $> 10^9$ pulses with less than 10% energy degradation have already been demonstrated at much higher energies and beam quality specs than required by OWL. In addition, while having the two OWL instruments conduct a laser scan over the region of an event, most of the cloud information would be obtained by a single instrument. Thus, the failure of one laser would not result in a significant loss of capability.

5.6 Spacecraft

OWL requirements on the spacecraft systems are relatively modest and the spacecraft is entirely conventional. The total wet mass of the spacecraft is estimated to be 1440 kg, leading to an all-up satellite weight of 3240 kg. Holding a 20% mass contingency the Delta 4050-H-19 can reach 5° inclination with 23% mass-to-orbit margin.

Pointing accuracy is about 2° with a knowledge of 0.01° . The satellite is three-axis stabilized using reaction wheels for attitude control and magnetic torque bars to damp momentum. Attitude and orbit determination uses an inertial reference unit, a star tracker, and GPS.

The propulsion system uses simple monopropellant hydrazine thrusters. During maneuvering, the propulsion system provides attitude control. This can also be used to provide a rapid slew to enter a safe-hold attitude pointing away from both the Sun and the Earth. Enough propellant is carried to enable orbit changing, station keeping, and end-of-life disposal.

When in daylight, the spacecraft is oriented so that the thermal radiators and one side of the spacecraft point to deep space and the solar array axis is normal to the sun-line. Single axis solar array drives point the array surface to the sun and 11 m^2 arrays can supply the needs of both spacecraft and instrument. The thermal system uses the cold side of the spacecraft to dissipate the estimated 430 W spacecraft bus power and two deployable radiators to dissipate the 600 W instrument power.

Space to ground communications use S-band and make use of a ground station at Malindi, with backup by Hawaii. With overhead, instrument and housekeeping data average 192 kbps during the viewing period and 12 kbps for the rest of the month. This buffered in a 256 Gbit solid-state recorder and a portion is telemetered each day. Two 6-minute data dumps per day are sufficient to downlink the full data volume. During early orbit acquisition and checkout TRDSS is used to provide near real-time data at 8 kbps and commanding at 2 kbps. Because there are no special viewing times or conditions, data latency is not critical and the method of data delivery can be chosen on the basis of cost and reliability.

Mission operations are largely autonomous and consist largely of monitoring the health and well-being of the instrument and spacecraft. These are easily supported by a PC-based ground station running commercial software and staffed on a 5 day 8 hour work week. Automatic alerts will be employed to signal anomalies. During early orbit operations and orbit changing maneuvers, mission operations will be staffed 24/7.

5.7 Viewing Efficiency

Conditions that prevent effective observation of UHECR showers include sunlight, moonlight, lightning, man-made light, oceanic biofluorescence, and high altitude clouds. Both the lights of civilization and the polar aurora make a high inclination orbit undesirable for OWL, and as a baseline we have adopted an orbit lying within

10 degrees of the equator. Each OWL eye must remain shuttered until the viewed Earth has entered full darkness, free from sunlight or moonlight. It then opens and after a finite interval (about 1 minute) can begin observations. Before re-entering the light (allowing enough time for the shutter to close), it ceases observations and closes its shutter. Requiring that the instrument only take data in full darkness, this results in an overall duty factor of 14.4%.

This duty factor is reduced further by man-made light, oceanic effects, lightning, and clouds. These are much harder to evaluate since they may affect only a fraction of the aperture. The frequency of global equatorial thunderstorm activity and of clouds above 3 km altitude, combined with an estimate of the effects of man-made light gives a reduction in efficiency of about 20% under the conservative assumption that these factors completely preclude observation in the affected region. This gives an overall efficiency of 11.5%. For high-energy events, the provision of an adaptive threshold may make it possible to improve this value by allowing "slowly" varying light sources such as lightning and man-made light to be tolerated.

The measurement efficiency of OWL for particular showers must take into account the effects of the position and orientation of the shower track relative to the detectors and the energy of the primary particle. The measurement efficiency will depend both on the trigger selectivity and the event reconstruction algorithms. These result in a complex energy-dependent efficiency that has its strongest effect near the detection threshold and rises to nearly 100% for higher energies. This has been examined using a Monte Carlo technique and is discussed below.

5.8 Monte Carlo Simulation

Crucial to OWL development are Monte Carlo simulations of the underlying physics and response of orbiting instruments to the UV air fluorescence signals. One such Monte Carlo has been developed at GSFC (Krizmanic et al., 2001). The simulation employs a hadronic event generator that includes effects due to shower starting point and development fluctuations, charged pion decay, neutral pion re-interaction, and the Landau-Pomeranchuk-Migdal (LPM) effect. Because the OWL baseline imaging requirements are rather insensitive to lateral shower size, the hadronic generator creates individual 1-dimensional shower parameterizations characterized as a 4-parameter Gaisser-Hillas function. Each air shower is developed in a sequence of fixed time intervals of 1 μ s and the resulting charged particles are used to generate air fluorescence and Cherenkov signals. The fluorescence signal is corrected for the pressure and temperature dependence of the atmosphere and large-angle scattering of the Cherenkov light into the viewing aperture of the instrument is accounted for. Once the UV light signal is generated, it is propagated out of the atmosphere to the orbit altitude including light losses by Rayleigh scattering and ozone absorption.

The response of the instrument is then considered. Response functions for the optical transmission and focal plane spot size as functions of shower viewing angle are based on the results of optical ray tracing modeling. The UV signal is attenuated by the filter response, mapped onto the focal plane array, and convolved with the wavelength response of a bi-alkali photocathode. The resultant pixel signals are Poisson fluctuated to obtain a photoelectron signal in each pixel for each time step. At the peak of a 10^{20} eV shower, the typical signal obtained in a single pixel crossing time (3.3 μ s) is 6 to 9 photoelectrons, depending on the location of the shower in the FOV. The background in the same time interval is about 0.6 photoelectrons. For $E = 10^{20}$ eV protons, preliminary event reconstruction results show an energy resolution of about 16 % and good X_{Max} resolution. Agreement to within 1° in

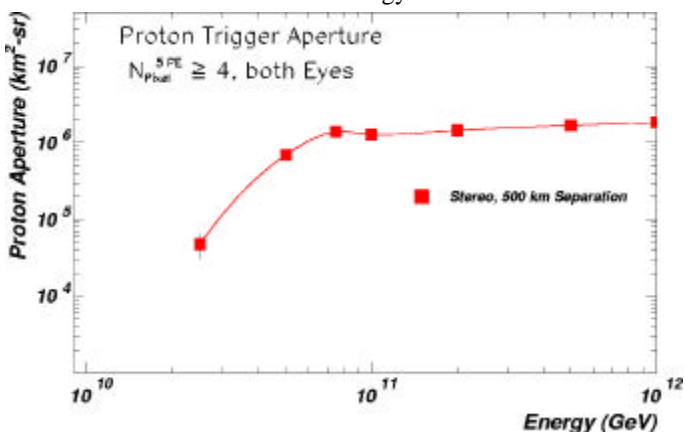


Figure 7

each view has been demonstrated generated shower tracks and tracks reconstructed using a moment-of-inertia method based on the amplitude measurements. This may be improved by incorporating timing information.

The ability of the baseline design to detect cosmic rays can be expressed in terms of an aperture ($\text{km}^2 \text{sr}$) as a function of incident cosmic ray energy. An isotropic flux of protons of a given incident energy is generated and the number of events accepted by a simulated event trigger is determined. This yields a detection aperture for a given particle energy, trigger, and orbit. Figure 7 illustrates the aperture as a function of energy for an altitude of 1000 km and a separation of 500 km. The asymptotic instantaneous aperture is $2 \times 10^6 \text{ km}^2 \text{sr}$.

References:

1. "Origin and Propagation of Extremely High Energy Cosmic Rays" by P. Bhattacharjee and G. Sigl, *Physics Reports* 327 (2000) 109.
2. "Observations of Implications of the Ultrahigh Energy Cosmic Rays" by M. Nagano and A.A. Watson, *Reviews of Modern Physics* 72 (2000) 689.
3. "Exploring the Ultrahigh Energy Neutrino Universe" by D.B. Cline and F.W. Stecker, astro-ph/0003459.
4. "The Curious Adventure of the Ultrahigh Energy Cosmic Rays" by F.W. Stecker, in "Phase Transitions in the Early Universe: Theory and Observations", ed. H.J. De Vega et al. (Dordrecht: Kluwer Acad. Pub.) 2001, p. 485, astro-ph/0101072.
5. "A Break in the Highest Energy Cosmic Ray Spectrum: a Signature of New Physics" by G. Sigl, S. Lee, D.N. Schramm and P. Bhattacharjee, *Science* 270 (1995) 1977 Astro-ph/9506118
6. "Workshop on Observing Giant Cosmic Ray Airshowers From $>10^{20}$ eV Particles From Space", Editors J.F. Krizmanic, J.F. Ormes and R.E. Streitmatter, AIP conference proceedings 433, 1998.
7. "Simulated Performance of the Orbiting Wide-angle Light-collectors (OWL) Experiment", J. F. Krizmanic et al., 27th- Int. Cosmic Ray Conference, Hamburg, 2001, 861